Optical Studies of the Conduction Band Offset at the $CdCr_2Se_4/Al_xGa_{1-x}As$ Interface

Jason Faulkenberry

Department of Physics, College of William and Mary, Williamsburg, VA 23187

(April 16, 2004)

ABSTRACT

$CdCr_2Se_4$ grown on a GaAs or $Al_xGa_{1-x}As$ substrate is a candidate for efficient spin injection necessary to exploit the spin degree of freedom in electrons for semiconductor devices. Recent measurements, however, have shown a very low spin injection efficiency, which is believed to be due to a paramagnetic state of the semiconductor, even in temperature regions when ferromagnetism is expected.

To measure the magnetic character of the absorption edge, or the energy band gap (E_g), a simple transmission/absorption measurement may be taken. The band gap of $CdCr_2Se_4$ is highly dependent on temperature, and below the Curie temperature should display ferromagnetic character, i.e. it should decrease with decreasing temperature due to the splitting of the spin bands. Measurements of the bandgap would help verify the relationship between the magnetism and the bandgap. As we see, however, other forms of absorption dominate, and this measurement cannot be made.

A second measurement that would help explain the poor spin injection is to measure the conduction band offset directly. The offset between the two layers can be measured by inducing a photocurrent and determining the threshold value. In this paper we measure the conduction band offset for light emitting diode samples, and detect very slight ferromagnetic character.

ACKNOWLEDGMENTS

First, I would like to thank my advisor Dr. Gunter Luepke for his constant support, encouragement, and patience, and for providing me with the opportunity to conduct this research project under his guidance. I have learned a great deal, both theoretically and experimentally while working on this project.

Next, I would like to acknowledge Dr. Qiguang Yang. I am indebted to him for his assistance throughout this experiment. Without his time, input and support, this research would not have been possible.

The author would finally like to thank the Chemistry Department at the College of William and Mary for supplying the FTIR equipment. I must also thank the staff at Jefferson Lab's Free-Electron Laser Facility of Newport News, for supplying workspace, as well as technical assistance. The author appreciates the assistance of Baozhou Sun with the laser system and setup.

A. Table Of Contents

1. INTRODUCTION

During the past few decades semi-conductor and electronics research has begun to take advantage of quantum mechanics in both design and function of semiconductor devices. However, up until the last few years, only traditional quantum mechanical aspects were focused on. Recently, the spin of the electron has been the focus of a new direction for research in electronics. This new field of spin electronics (often known simply as spintronics) attempts to utilize the spin degree of freedom in the electron to create devices instead of the more traditional focus on charge [1,2].

In order to exploit the spin degree of freedom in the electron it is necessary to be able to efficiently inject carriers with polarized spin from a ferromagnetic contact into a semiconductor [3]. In order to create high efficiency in spin injection, a number of conditions must be met. First, the ferromagnetic material chosen must have a high spin polarization. Second, it is necessary to have an appropriate interface between the ferromagnet and the semiconductor. Recent calculations have shown that a large band offset between the contact and semiconductor often prohibits efficient spin injection [4]. Finally it is necessary to have strong magnetization at the ferromagnet/semiconductor interface.

One promising candidate is n-type $CdCr_2Se_4$, a ferromagnetic semiconductor (FMS) that has been grown on a GaAs or $Al_xGa_{1-x}As$ substrate [5]. Dr. Jonker's group, of the Naval Research Laboratory, has demonstrated epitaxial growth of n-type $CdCr_2Se_4$, a chalcogenide spinel FMS, on both GaAs and $Al_xGa_{1-x}As$ (as in our samples), as well as GaP [5]. $CdCr_2Se_4$ displays all of the conditions mentioned above that are required for efficient electron spin injection. Above the Curie Temperature T_c = 130 K [6], it displays paramagnetic properties typical of a nonmagnetic semiconductor, the absorption band edge decreases with an increasing temperature; but below the Curie temperature it enters a ferromagnetic state and the absorption band edge decreases with a decreasing temperature (Fig. 1).

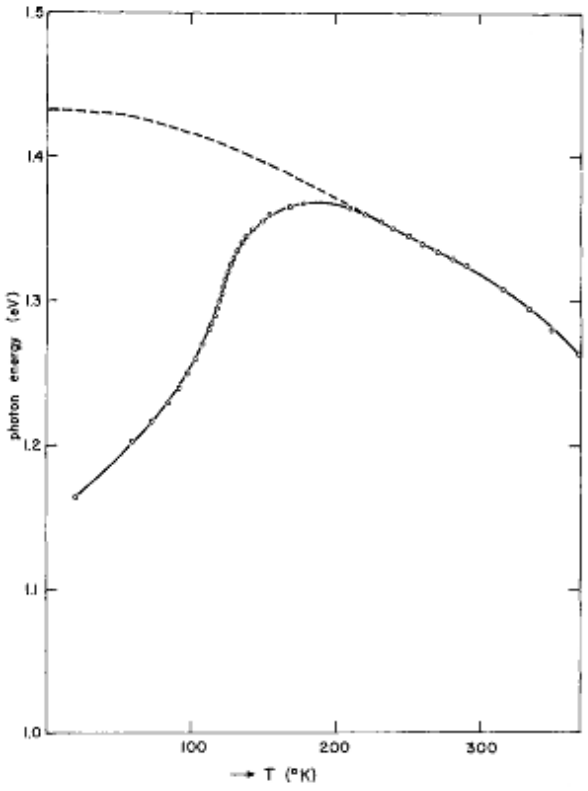

FIGURE 1. Energy Gap of $CdCr_2Se_4$ versus temperature. Dashed line: assumed extrapolation for paramagnetic state [7].

The magnetic moment in the $CdCr_2Se_4$ crystal comes primarily from the Chromium atoms. The magnetic moment of the Cadmium atom is very low, while the Selenium is small and opposing that of the Chromium. The Chromium atom, however, has almost thirty times the magnetic moment of Selenium, and thus contributes almost the entire magnetic moment of the crystal (Fig. 2).

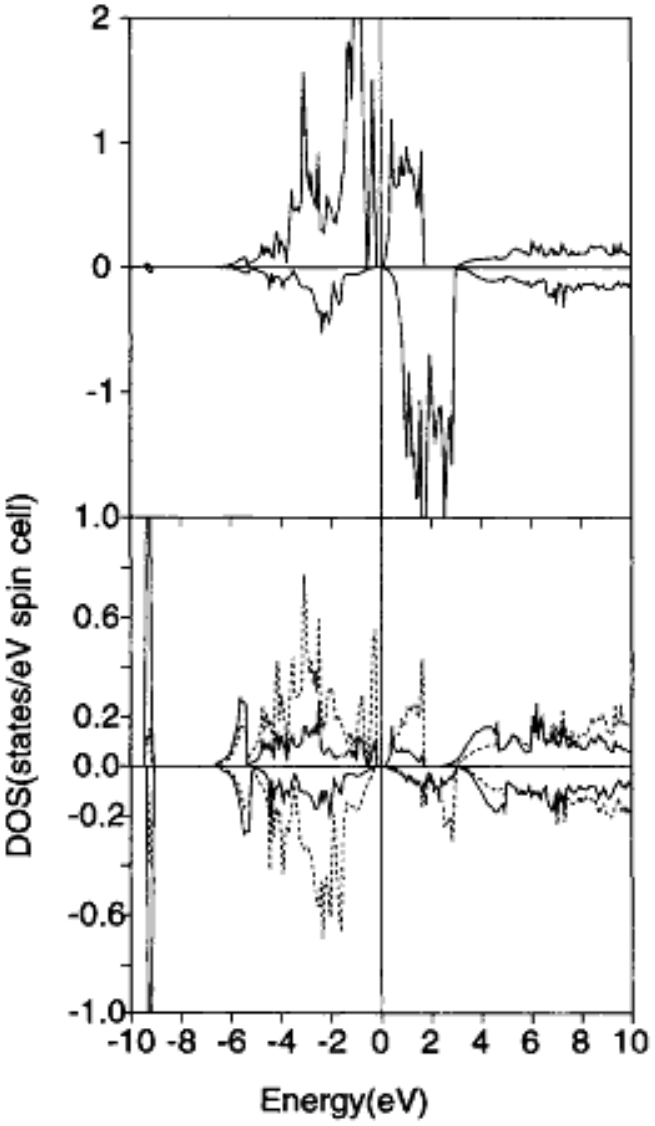

FIGURE 2. Majority and minority component of the projected density of state for Cr (upper panel) and Cd and Se (lower panel), solid and dashed lines, respectively [8].

The conduction band offset is rather large, at least at room temperature [3]. A simple threshold estimate gathered from the photocurrent spectrum of $CdCr_2Se_4/Al_{0.09}Ga_{0.91}As$ showed the conduction band offset, ΔE_C, to be 660 meV (Fig. 3) [3]. This is undesirable as it can cause electron scattering due to high kinetic energy, precluding efficient spin injection [9].

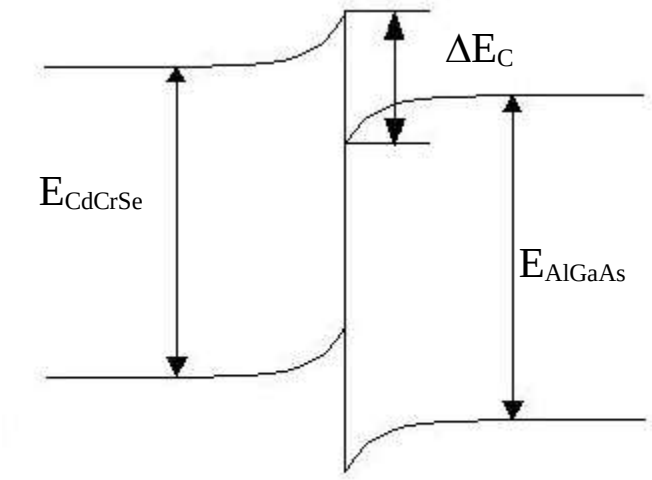

FIGURE 3. Energy Gaps at the interface of the of CdCr2Se4/AlGaAs heterostructure [3].

The conduction band offset is expected to have strong temperature dependence, particularly below T_c. GaAs, $Al_xGa_{1-x}As$, and $CdCr_2Se_4$ all demonstrate an increasing band gap with decreasing temperature above T_c, but below the Curie temperature, as mentioned above, $CdCr_2Se_4$ enters a ferromagnetic state. As the band gap of $CdCr_2Se_4$ decreases (Fig. 1), the fundamental gaps of GaAs and $Al_xGa_{1-x}As$ increase, thus the conduction band offset would be assumed to decrease.

In the samples we studied some were measured to have slight ferromagnetic characteristics, while others were measured to be paramagnetic. But even in the samples that displayed ferromagnetism the spin injection efficiency has been very low (<6%) [9].

In order to understand the cause of the inefficiency it is necessary to have a better understanding of the interface, band gap, and the band offset between $CdCr_2Se_4$ and the substrate, ideally with respect to temperature. We investigated the band gap and band offset in this work.

We first set out to measure the absorption edge of the $CdCr_2Se_4$ as a function of temperature. This would characterize the magnetization of $CdCr_2Se_4$ in the heterostructure, and could be compared to intrinsic $CdCr_2Se_4$. This measurement could help to explain the poor spin injection efficiency. As long as the substrate is transparent, this can be done using a simple transmittance measurement on a spectrometer in the region of about 5,000 cm^{-1} to 20,000 cm^{-1}.

In addition to the direct measurement of the absorption edge, the conduction band offset between the $CdCr_2Se_4$ and the substrate was measured. This can give direct clues regarding the poor spin injection efficiency. There are numerous techniques for this type of measurement, and in this work we used a Titanium:Sapphire laser system, which provides high-power tunable radiation to produce a measurable photocurrent in the diode samples.

2. THEORY

$CdCr_2Se_4$ like any crystal has different energy levels that are allowed for the electrons in the lattice, commonly referred to as energy bands (Fig. 5). Between these allowed energies, or bands, are forbidden regions, known as energy gaps, or band gaps. An electron is (typically) not allowed to exist in these regions, and when absorbing energy must have enough energy to overcome the gap. In an atom, the outermost level of electrons that interact with other atoms but are still bound is known as the valence band. The top energy level of the valence band is typically defined as zero. The conduction band is the energy level in which electrons behave like free particles, and have enough energy to move around the crystal structure. The energy difference between the highest energy of the valence band and the lowest energy of the conducting band is known as the fundamental band gap [10].

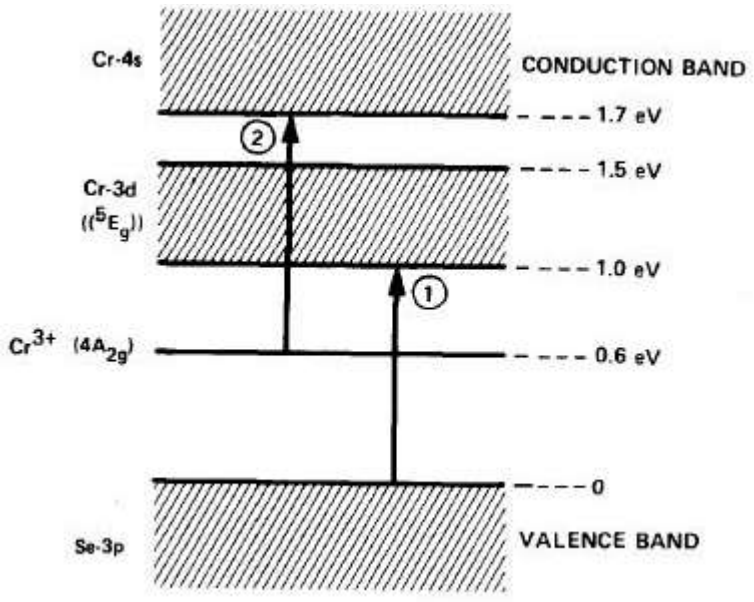

FIGURE 4. Band structure of $CdCr_2Se_4$ [11].

In $CdCr_2Se_4$ the d bands exist in the fundamental gap of the crystal (Fig. 5). It is important to note that electrons can be excited to the d bands, and therefore the crystal can absorb energy below the band gap, this is known as the absorption edge.

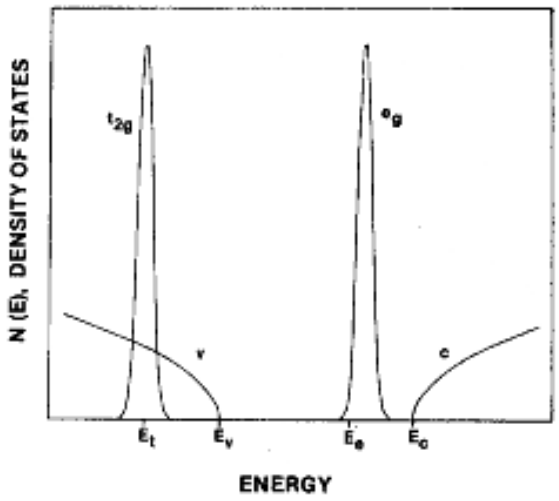

FIGURE 5. Schematic electronic structure of CdCr2Se4 based upon photoemission and optical measurements. Only the parallel-spin d bands are shown. The fundamental gap is Ec-Ev. For CdCr2Se4 Ec-Ev is 1.45 eV. The absorption edge is given by Ee-Ev[12].

When a sample such as $CdCr_2Se_4$/GaAs or $CdCr_2Se_4$/AlGaAs is grown, there are typically deliberate impurities added, termed doping. The doping is either n-type or p-type depending on whether the impurities added to the crystal lattice are electron acceptors or electron donors. In a crystal lattice an atom forms a certain number of bonds with nearby atoms, depending on its position, and its number of valence electrons. When an atom has fewer valence electrons than required to create bonds then a deficit is formed in the lattice, which is typically referred to as a hole, and reacts with the lattice as a

charged particle with the mass of an electron, but with a positive charge. If the acceptors are dominant in a lattice, then holes are released in the valence band of the crystal. The opposite doping is also possible. Atoms with more than the required electrons are introduced to the lattice, and can release their electrons into the lattice in the conduction band, so that electrons are always present in the conduction band. These are known as carriers and behave like free electrons.

These electrons, typically known as free carriers, along with electrons in the valence band are typical causes of absorption; but there are others. The following figure demonstrates four typical types of absorption in semiconductors.

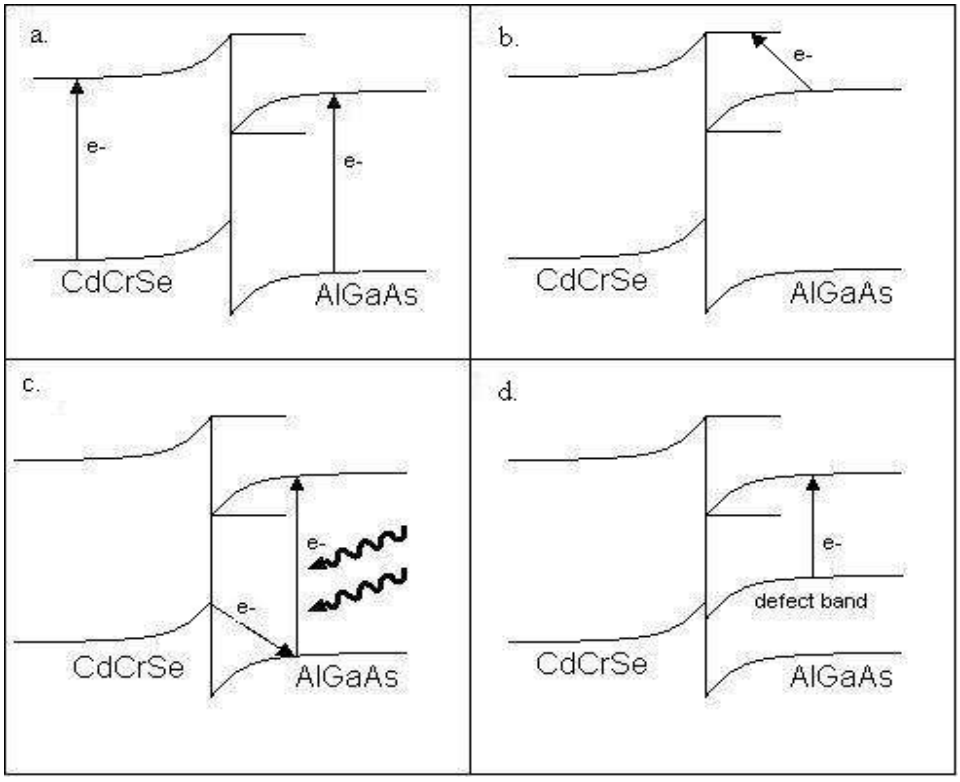

FIGURE 6. Major types of absorption in semiconductors. For details see text.

Figure 6 (a) demonstrates typical band gap absorption, from both the substrate, and the $CdCr_2Se_4$ layer. The electrons absorb energy from a photon and move from the valence band to the conduction band. Figure 6(b) displays the mechanism for electron injection across the band offset. Electrons in the conduction band of the substrate are excited from the conduction band of the AlGaAs layer to the conduction band of the $CdCr_2Se_4$. In addition to these types of absorption, which were the desired types in our experiments, there can be also two-photon absorption (Fig. 6(c)). Two-photon absorption occurs when the valence electrons in the substrate are excited by two photons and make the jump across the band gap. Finally there may be defect absorption (Fig. 6(d)). Defect absorption occurs when defects in the sample create an energy band that lies within the band gap of the sample. In this way, photons with energy smaller than the difference in the band gap can still excite electrons into the conduction band. However, in our samples the defect absorption was negligible.

Classical electromagnetic theory is used to treat the absorption and transmission data with regard to the absorption gap. Assuming the setup demonstrated in Figure 4, where I_{in} and I_{out} are the intensity of the incoming and outgoing light respectively, the following steps are used to determine the

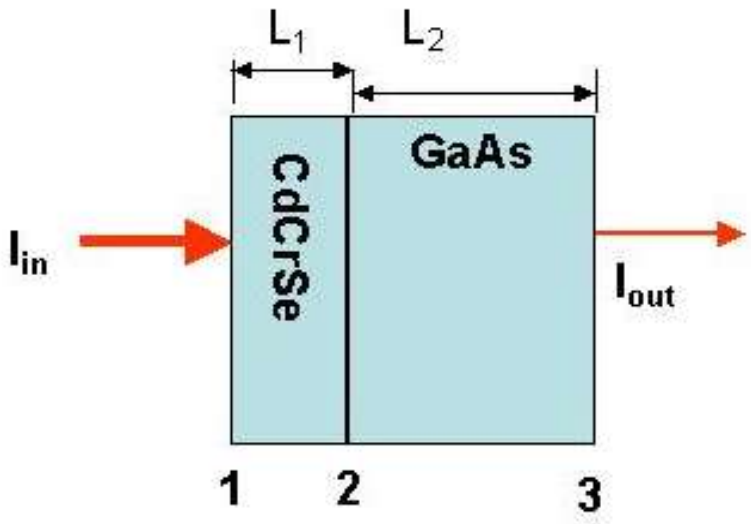

FIGURE 7. Diagram of radiation incident on the $CdCr_2Se_4$/GaAs crystal [13].

free carrier absorption [13]. First we define the absorption of the $CdCr_2Se_4$ layer as:

$$\alpha_{Cd} = \alpha_{Cd}^{\ bandgap} + \alpha_{Cd}^{\ other}, \tag{1}$$

where α_{Cd}^{other} is the absorption from the $CdCr_2Se_4$ layer other than the band gap, such as free carriers, which we will see has a large effect on the total absorption. We neglect multiple-reflections and note that the transmission, T, is

$$T = \frac{I_{out}}{I_{in}} \propto \exp(-\alpha_{Cd}^{\ bandgap} L_1 - \alpha_{Cd}^{\ other} L_1 - \alpha_{sub} L_2), \tag{2}$$

where α_{sub} is the absorption of the substrate (in this case GaAs). Thus from a transmittance measurement, if

$$\alpha_{Cd}^{\ other} L_1 + \alpha_{sub} L_2 >> \alpha_{Cd}^{\ bandgap} L_1, \tag{3}$$

then one cannot gather any information of the band gap because the free carrier absorption and the substrate absorption account for the majority of the absorption of the heterostructure, while the absorption from the bandgap is on the level of noise.

As shown in Figure 3, the valence and conduction bands do not line up in the $CdCr_2Se_4$/AlGaAs heterostructure. The fundamental gap of AlGaAs is 1.54 eV and $CdCr_2Se_4$ is 1.3 eV at room temperature; but the conduction band of $CdCr_2Se_4$ is higher in energy than in AlGaAs [3]. To measure the band offset, $\Delta E_{C,}$ electrons from the conduction band of the substrate are excited to the conduction band of the $CdCr_2Se_4$ layer. In a diode structure the electrons may be excited from electromagnetic radiation, inducing a photocurrent. Typically a light source of variable frequency is used, and the photocurrent generated is measured around the expected threshold energies. The photocurrent can be plotted as a function of the photon energy to determine ΔE_C.

When ΔE_C approaches half of the fundamental gap, a photocurrent can be generated both by exciting electrons from the conduction band of the GaAs substrate, and by exciting electrons from the valence to the conduction band of $CdCr_2Se_4$ or the substrate through two photon absorption. When the input energy is below half of the band gap, two-photon absorption is negligible, but for our samples becomes noticeable around $\Delta E_{C.}$ For a pulsed high-intensity photon source, two-photon absorption is characterized by the equation,

$$\Delta n = [\alpha(\omega) I_{\omega}^{m} + 0.5\beta(\omega) I_{\omega}^{2}]\tau_{p}(\hbar\omega)^{-1} \tag{4}$$

where Δn is the photo induced population change of electrons per unit volume, alpha,

beta, τ_p, and h-bar*ω are the one and two-photon absorption coefficients, the width of the laser pulse and the incident photon energy respectively [14]. The exponent m is typically in the range of 0.5 to 1.0. It is important to note that at higher intensities two-photon absorption plays a much larger role in the absorption process, while at lower intensities single photon absorption dominates.

3. EXPERIMENT

3.1 Samples

We used two different types of samples for our experiment. The first was a simple heterostructure, much like the diagram shown in Figure 7. In this structure, a layer of $CdCr_2Se_4$ is grown on a substrate of GaAs or AlGaAs. The substrate can be intrinsic or it can be doped either n-type or p-type. We used this type of sample in our FTIR measurements.

The second type of sample is a light emitting diode (LED) heterostructure. In these LED structures a number of layers of GaAs or AlGaAs are grown on top of each other with different dopants, and with a final layer of $CdCr_2Se_4$ grown on top. An example of a typical LED structure is shown in Figure 8.

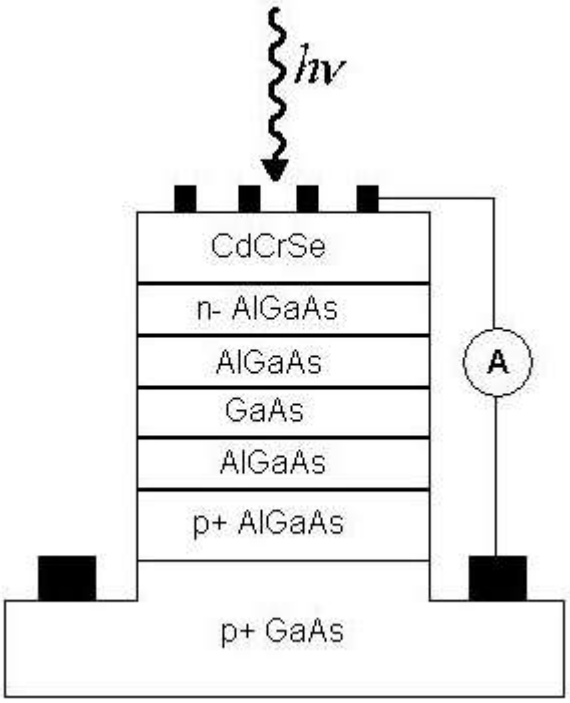

FIGURE 8. Diagram of a typical light emitting diode sample [3]

3.2 Fourier Transform Infrared Spectrometry

The first goal was to measure the fundamental band gap of $CdCr_2Se_4$ at varying temperatures. The idea was to correlate the ferromagnetic behavior of the $CdCr_2Se_4$ layer, which was measured independently by SQUID measurements, with temperature dependence of the bandgap. Electronic transitions across the band gap will yield a small increase in the infrared absorption. We decided to use a Fourier Transform Infrared (FTIR) spectrometer to measure the fundamental gap of $CdCr_2Se_4$. FTIR Spectroscopy is based on the idea that radiation absorbed in a material can provide specific information about the chemical, electronic, and structural properties. In some cases a spectrum from a material may contain discrete lines or bands, and in other cases it may contain a continuum. Each feature can be identified and associated with a particular atom, molecule, or structure and its environment. The FTIR spectrometer is based on the Michelson interferometer. Figure 9 illustrates a typical setup of a Michelson interferometer. The source can be either monochromatic or broadband, and is passed through a beam-splitter, which ideally transmits 50% and reflects 50%. Half of the light is passed to a stationary mirror while the other half is passed to a moving mirror. The reflected and transmitted light are recombined at the beamsplitter and then passed to a detector.

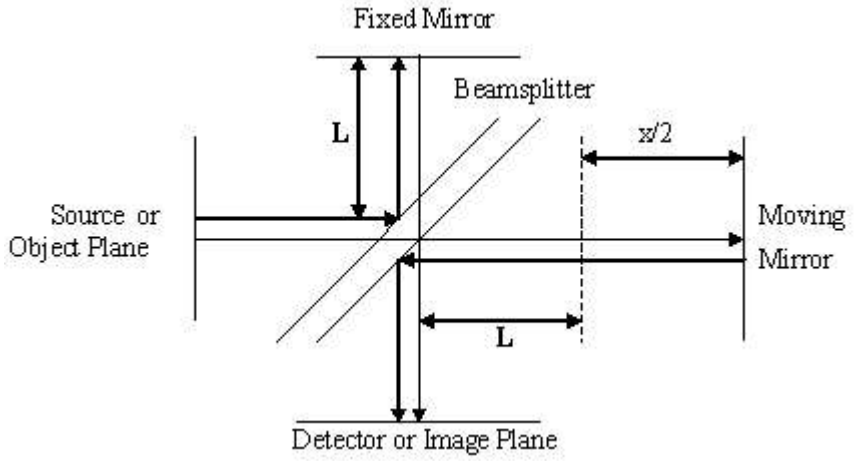

FIGURE 9. Basic layout of a Michelson Interferometer.

For monochromatic light this gives a two-beam interference relation for the intensity, where the input light has a wavenumber k_0 and intensity $B(k_0)$, while the path difference for the two waves is x [15]

$$I_0(x) = B(k_0)[1 + \cos(2\pi k_0 x)] \tag{5}$$

The preferred measurements of radiation are made in relation to the wavenumber k. Typically the wavenumber is measured in units of cm^{-1} which is related to both the wavelength, λ, and the frequency, ν, of the radiation by $k = (1/\lambda) = (\nu/c)$. The intensity of the output can be generalized to a broadband spectrum, and becomes

$$I_0(x) = \int_0^\infty B(k)[1 + \cos(2\pi kx)]dk \tag{6}$$

This is simply a superposition of cosine waves, creating an interference pattern. At pathlength zero, all wavelengths are in phase and add constructively. However as the path length is changed by varying the position of the moving mirror, an interference

pattern emerges that is known as an interferogram. When the mean value of the interferogram is subtracted from the function, then the intensity of the output can be measured as a function of the path difference x,

$$I(x) = I_0(x) - \overline{I(x)} = \int_0^\infty B(k)\cos(2\pi kx)dk \tag{7}$$

The interferogram produced by this method contains all the frequencies of the radiation from the source, superimposed on one another. This is actually the cosine Fourier transform of the source distribution, I(k), which is what we are interested in. In order to get I(k) we take the inverse Fourier transform of the interferogram by

$$B(k) = \int_0^\infty I(x)\cos(2\pi kx)dk \tag{8}$$

The result is a spectral distribution with the intensity measured as a function of wavenumber, k, instead of path difference. It is also necessary to take a background spectrum, $I_b(k)$, without any sample, and compare this with the sample spectrum, I(k). This results in the absorption spectrum, calculated as

$$Abs(k) = -\log_{10}\frac{I_B(k)}{I(k)} \tag{9}$$

The resulting absorption spectrum is plotted on a log scale. This procedure has the added bonus of removing absorbance peaks inherent in the spectrometer from gases and other materials that are always present.

3.3 Optical Parametric Amplifier System

In order to measure the conduction band offset, Free Carrier Absorption by Internal Photoemission was implemented using a picosecond Optical Parametric Amplifier (OPA) laser system. An OPA splits one high frequency photon provided by the pump beam into two lower energy photons, a signal beam and an idler beam. This is accomplished by use of a nonlinear crystal. In our setup a Beta Barium Borate (BBO) crystal was used. Due to material dispersion, energy and momentum cannot both be conserved for most directions of propagation through the crystal. However, there is a range of propagation angles where energy and momentum are conserved. Rotating the crystal in this range allows the tuning of the frequencies of the signal and idler waves. A very simplified diagram of the OPA setup is shown in Figure 10.

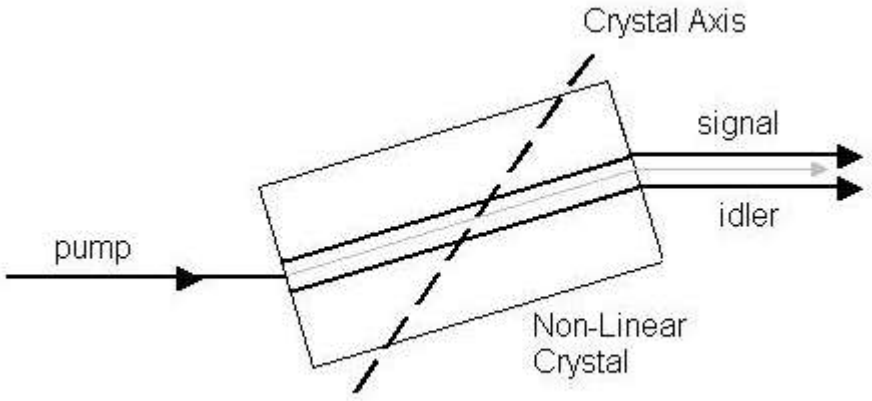

FIGURE 10. Basic setup of the optical parametric amplifier laser system

There were two setups used for this part of the experiment, the basic setup is shown in Figure 11.

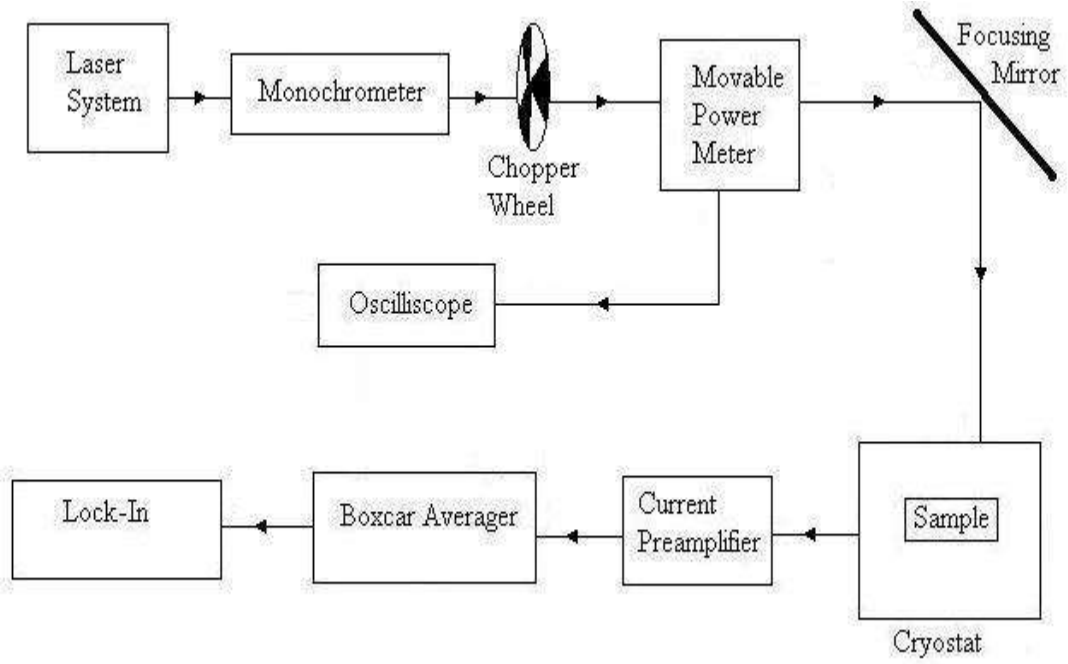

FIGURE 11. Experimental setup for the band-offset measurement.

In the first setup neither the monochromator nor the chopper wheel was used; and instead of the Lock-In a simple multimeter was used. The laser beam was directed first to a power meter, so the input intensity could be calculated and kept constant during the measurement. The power meter was then removed and the beam was focused onto the sample, which was located in a cryostat, so that the measurements could be made at different temperatures. The sample in the cryostat was connected to a current preamplifier, to increase the signal from the induced photocurrent. The output signal (after the preamplifier) was sent into the boxcar averager. A boxcar averager is an electronic device used to integrate a short signal over a narrow time window (gate),

thereby reducing the average noise. The boxcar averages the photocurrent signal over several laser pulses. The output from the boxcar is recorded on the computer. The second setup was designed in order to measure the photocurrent at lower intensity thereby reducing the two-photon absorption, and decreasing the noise. The second experimental setup is displayed in Figure 11. The laser beam first passes through a monochromator. A monochromator is a device that makes use of Bragg's equation,

$$\lambda = 2d \sin\theta \tag{10}$$

In a monochromator the incident beam is directed to a grating, with spacing between grooves of d, and an incident angle of θ. A beam of the desired wavelength is reflected back at an angle of 2θ. This serves to remove ambient light, and secure a single wavelength signal. It is then passed through a chopper wheel used for lock-in detection.

The lock-in is a device used to increase the signal-to-noise ratio. The first requirement to effectively use a lock-in is that the signal be modulated at a known frequency; the chopper wheel provides this necessary modulation. The known frequency of modulation is used as a reference signal that may be phase shifted. The modulated signal is passed through an amplifier to increase the signal to a level that can be sent through a demodulator. The demodulator, also known as a mixer, multiplies the input signal and the reference signal together. If the input signal is written as $\upsilon_0 A\cos(\omega_0 t)$, where A is the gain from the amplifier, $2\omega_0$ is the chopper frequency, and t is the time, and the phase-shifted reference is written as $\cos(\omega_0+\gamma)$, then the product is,

$$\upsilon_0 A\cos(\omega_0 t)\cos(\omega_0 t+\gamma) = \frac{\upsilon_0 A}{2}[\cos(2\omega_0 t+\gamma)+\cos(\gamma)] \tag{11}$$

This output signal consists of both a relatively high frequency signal at $2\omega_0$, and a DC signal. Finally, the signal is passed through a low pass filter to remove the high frequency signal. The output of the low pass filter is $\upsilon_0 A\cos(\gamma)/2$. The reference signal is phase shifted to provide the maximum output.

In both setups the temperature was varied between 80 K (liquid nitrogen) and room temperature through the use of the cryostat. This allowed the measurement of the effect of temperature on the conduction band offset.

4. RESULTS AND DISCUSSION

The primary difficulty in obtaining absorption and transmission measurements results from unwanted absorption of the free carriers and the substrate. The original samples that were sent to us from Dr. Jonker's group were less than 1μm thick n-type $CdCr_2Se_4$ grown on an AlGaAs or GaAs substrate (Fig. 7). In these samples the effective absorbance (A) was measured through a transmittance (T) measurement. This included absorbance from the substrate and from other sources (we included scattering because it also leads to a loss of the light intensity). From equation 9, A = -log T, and the absorbance for our samples was measured to be larger than 8 [13]. Then applying equation 2 (and neglecting band gap absorption),

$$\alpha_{Cd}^{\ other} L_1 + \alpha_{sub} L_2 = -\ln T = A \ln 10 = 2.3\, A\,. \tag{12}$$

This value for our samples was greater than 18. As noted earlier, if this is much greater than the band gap absorption then no information can be gathered about the absorption gap. Absorption for bulk $CdCr_2Se$ (α_{CD}) at 1.3 eV is about 10^5/m, but the thickness is less than 1μm (L_1), thus the contribution to the absorbance of the sample due to the band gap ($\alpha_{CD}^{\ bandgap} L_1 < 0.1$) is much less than the contribution from other sources[13]. Because this is around the level of noise, no information about the band gap can be gathered from the spectral distribution. The absorption due to the free carriers has to be removed if the measurement of the band gap is going to be determined from the spectrum. We requested new samples of $CdCr_2Se_4$ grown on a substrate of intrinsic GaAs in the hopes that the absorption would be smaller.

The absorption measurement of these two samples in the range 500 to 5000 cm-1 (Figs. 12 and 13), do indeed demonstrate a smaller absorption. There is almost a thirty percent reflection at each surface, so the best that could be hoped for is a forty percent transmittance, or about 0.4 optical density. The two samples for much of the spectrum stay around an optical density of 1, or ten percent transmittance, with an increase in absorption at higher wavenumbers. Ten percent is still enough to produce an interference pattern. It must be noted however, that the range we were interested in was higher in wavenumber than this spectrometer could measure. But when the spectrum taken is examined it demonstrates a trend toward increasing absorption at higher wavenumbers. The samples should actually become more transparent as the wavenumber gets larger. The first sample had approximately one percent or less transmission at the end of range

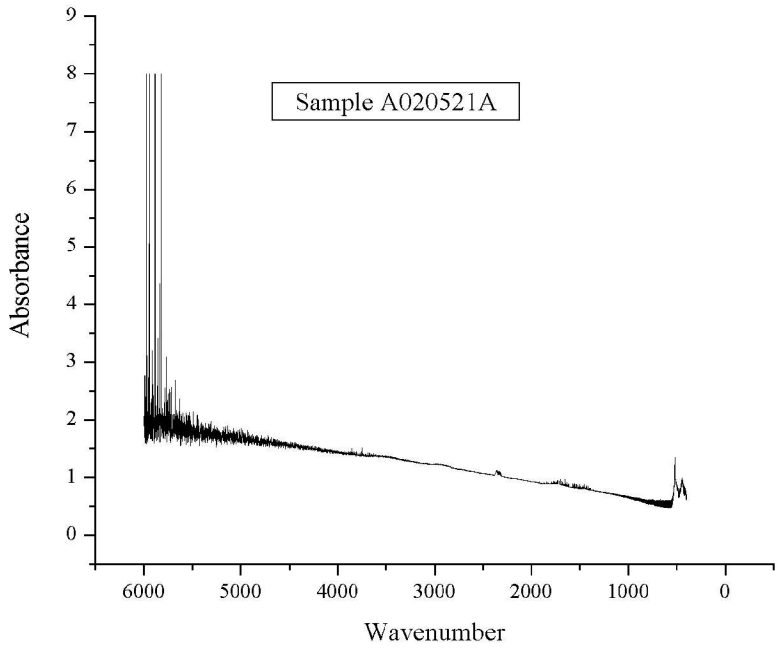

FIGURE 12. Absorption Spectrum of $CdCr_2Se_4$/GaAs sample A020521A.

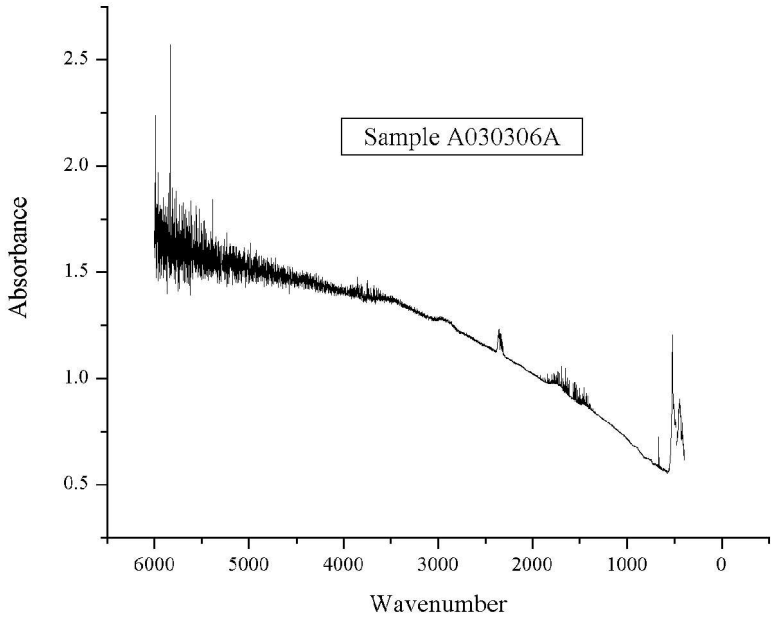

FIGURE 13. Absorption Spectrum of $CdCr_2Se_4$/GaAs sample A030306A.

of the band gap, and with the continuing trend, would soon have a signal too small to measure. The second sample had a slightly higher transmission, although still small, at around two to three percent. This sample also displayed a trend of increasing absorption, which would again prevent a successful measurement in the band gap energy range.

We decided to get around this problem by increasing the intensity. We also changed the technique and focused on measuring the band offset instead of the band gap. The increase of intensity was accomplished using a picosecond OPA laser system. We obtained several diode samples, but only a few of them had low enough resistance to allow useful measurements. We measured two samples, diode #11 and diode #13. Diode #11 had previously displayed some ferromagnetic properties with respect to the electron

spin injection, while diode #13 appeared to be paramagnetic. Diode #11 had demonstrated little change in spin injection efficiency with a decrease in temperature, and was therefore described as ferromagnetic. It is important to note that Diode #11's injection efficiency, while higher than diode #13, was still only around 6 percent. This would indicate, perhaps only 10% ferromagnetic character. The following graphs show the data taken at 300 Kelvin and 80 Kelvin respectively, for diode #11.

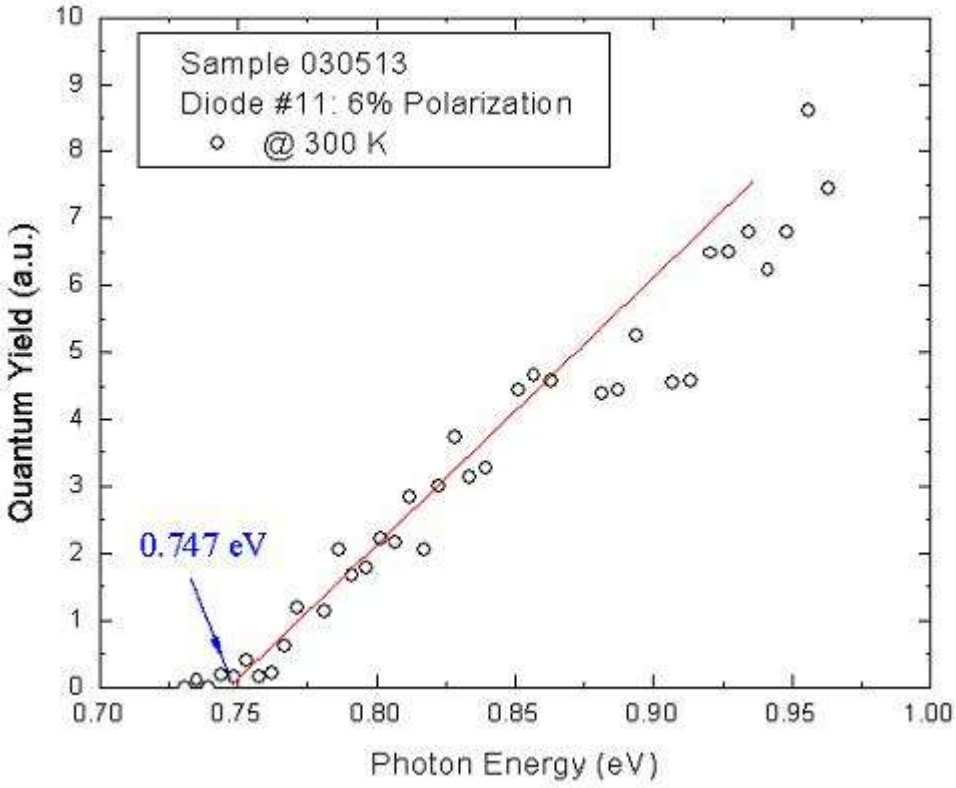

FIGURE 14. Photocurrent measurements of diode #11 at 300K.

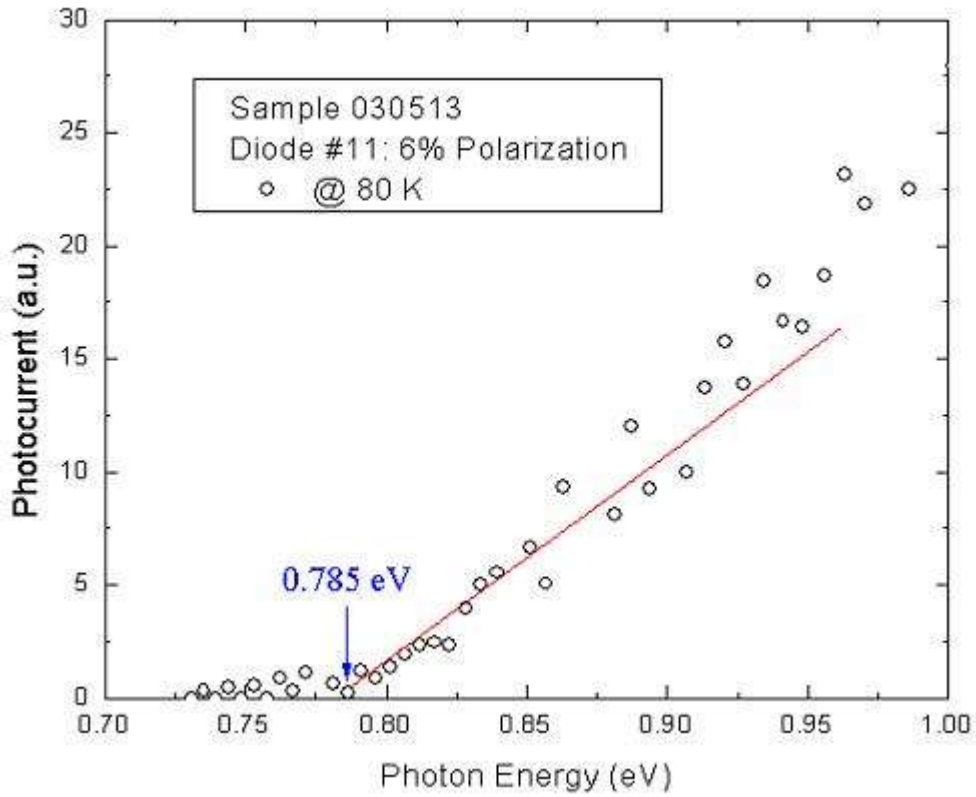

FIGURE 15. Photocurrent measurements of diode #11 at 80K.

Figures 14 and 15 show the photocurrent from the $CdCr_2Se_4$-AlGaAs heterostructure measured at room temperature and 80 K respectively. The thresholds in the photocurrent exhibit a band offset of 0.747 eV at room temperature and 0.785 eV at 80 K. The increase in the band offset with a decrease in temperature again demonstrates the lack of expected ferromagnetism.

The second sample (diode #13) measured was a paramagnetic sample that could then be compared with diode #11. Preliminary measurements, made without the Lock-in, displayed a band offset increasing with a decrease in temperature. This is the expected behavior of this paramagnetic sample, although it actually behaved very much like the supposed ferromagnetic sample.

At this point there was a possibility that the photocurrent was actually caused by two-photon absorption, instead of from the band offset, which would render the measurements useless. This was especially worrisome because of the high-powered light source. As noted earlier two-photon absorption is non-linear with respect to the intensity. To test this, an intensity dependence measurement was taken. A simple curve of the form $y=a*x^b$ could be fitted to this data. Ideally, the curve would be linear, but if b were closer to 2, it would indicate that two-photon absorption is the dominant absorption process. We made preliminary intensity dependence measurements of sample #13 at 300K for the wavelengths of 1300 nm and 1500 nm. The curves fit to this data did not indicate a linear dependence. In the regime of the band offset energies (1300 nm) b was approximately 1.4; while at 1500 nm, it was about 2. This was indicative of two-photon absorption.

In order to decrease the two-photon absorption, it was necessary to decrease the intensity of the laser. The difficulty with lowering the intensity was that if it was too low, the photocurrent could become too low to measure. A Lock-In was therefore employed to increase the signal to noise ratio, in the hopes that we could then decrease the intensity enough to make the two-photon absorption negligible. The following graph shows the intensity dependence after the implementation of the Lock-in with lower incident intensity.

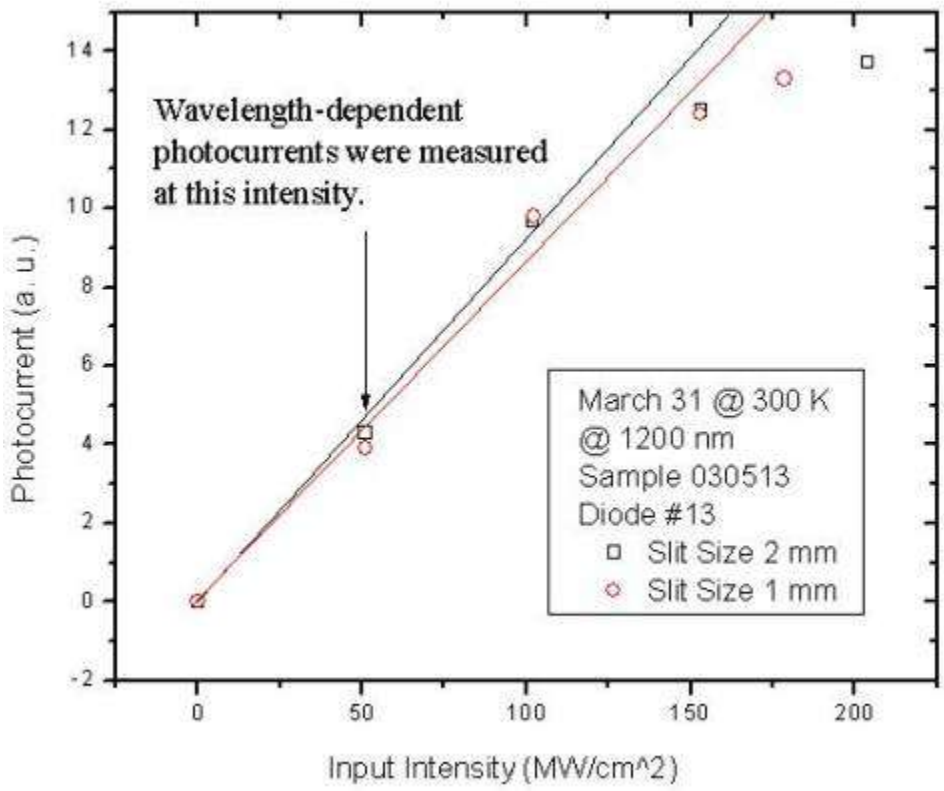

FIGURE 17. Intensity dependence of diode #13.

As mentioned above, we want the intensity dependence to be linear; therefore later measurements were made in the regime where the intensity dependence was as close to linear as possible (around 51 MW/cm^2 at 300K). Using equation 4, we can estimate the contribution from each type of absorption. For diode #13, at 51 MW/cm^2 laser intensity, the two-photon absorption is only about 12%, while the single photon absorption is about 88% of the total absorption. At 80K and 19 MW/cm^2 two-photon absorption counted for 25%, while single-photon absorption counted for 75%. We can see that the single photon absorption is the dominant process in this regime. Using these intensities we were thus able to measure the band offset. Because this intensity is small the Lock-in was again used to increase the signal to noise ratio. The following graphs show the data taken at 300K and 80K at the above intensities.

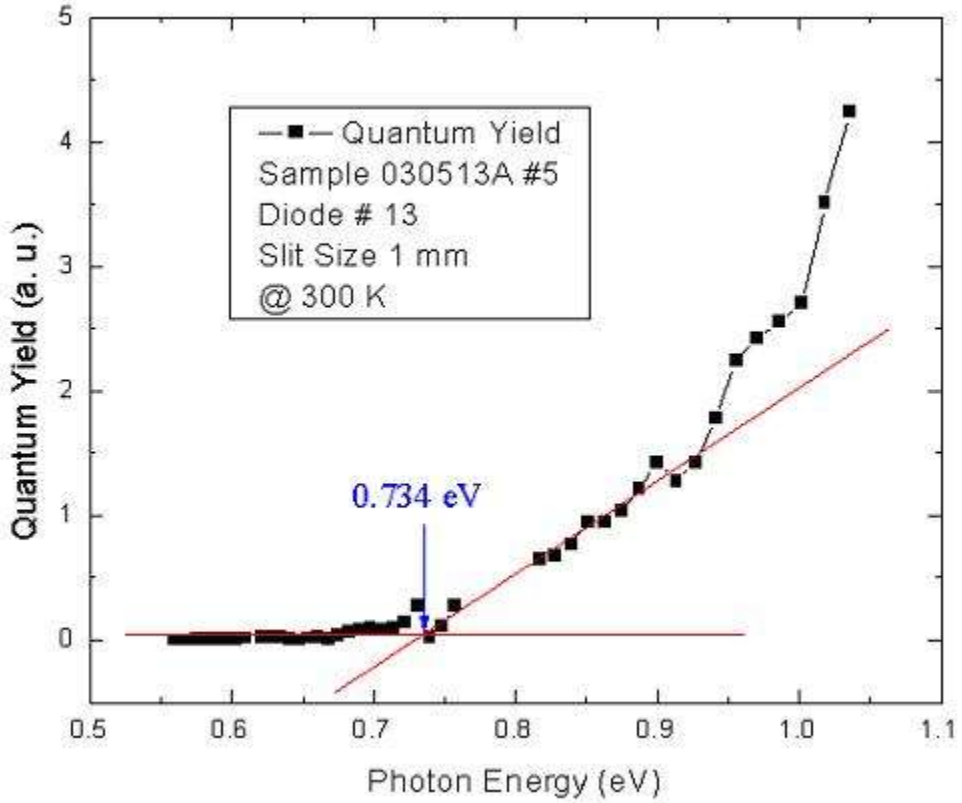

FIGURE 18. Photocurrent measurements of diode #13 at 300K, lower intensity, with Lock-in.

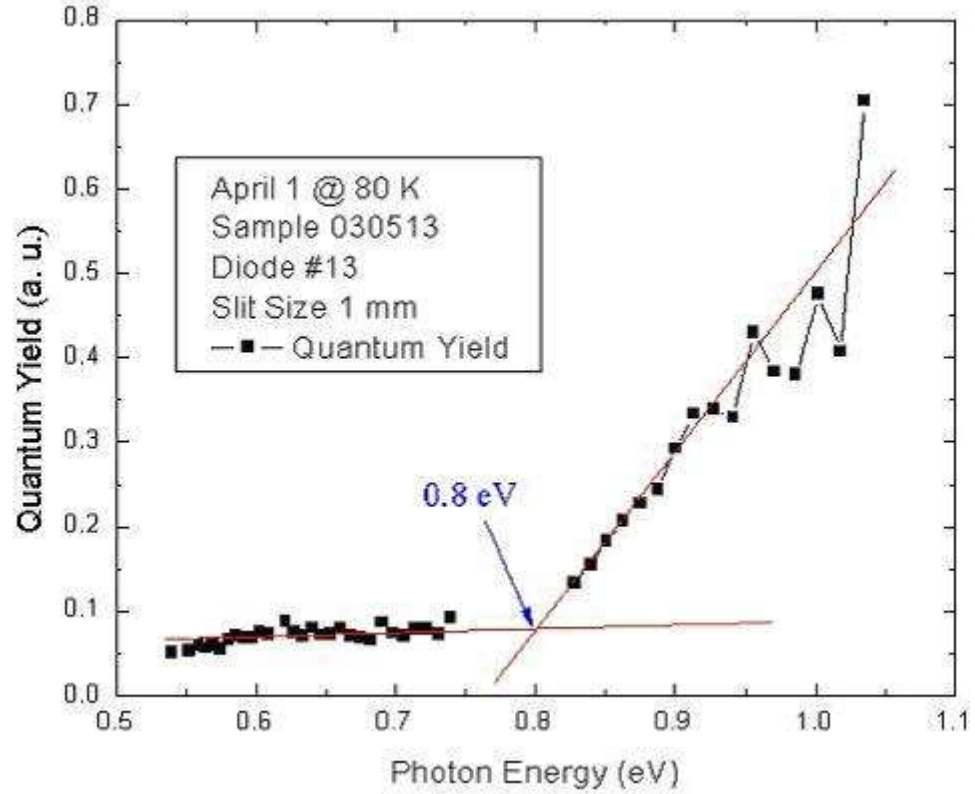

FIGURE 19. Photocurrent measurements of diode #13 at 80K, lower intensity, with Lock-in.

The band offsets have again been noted in the figures as 0.734 eV at 300K and 0.8 eV at 80K. Table I displays the measured values for the two samples.

Diode	300 K	80 K
11	0.747 eV	0.785 eV
13	0.734 eV	0.8 eV

TABLE I. Band offsets for diodes #11 and #13.

Table I shows that the band offset for both samples increase with a decrease in temperature. This is typical paramagnetic behavior. However when compared, it is noted that the change in band offset for the ferromagnetic diode is slightly smaller. This may be one of the few indications of the ferromagnetism of diode #11. The ferromagnetism allows some band splitting, which causes the band offset to increase more slowly. Even with this, however, the splitting is very small, and thus the ferromagnetic sample displays only a very small amount of ferromagnetic character.

It can be thus concluded that the ferromagnetism of sample #11 does affect the band offset. It can also be shown to be very slight. This is most likely due to a mixed interlayer between the $CdCr_2Se_4$ and the AlGaAs substrate that destroys most of the expected ferromagnetism. To test this, more samples would need to be grown, and the band offsets must be characterized for a larger number of diodes.

5. CONCLUSIONS AND FUTURE WORK

There are numerous difficulties in these measurements. And in fact, each of the different measurements taken provided different obstacles. In the FTIR measurements we discovered that the highly doped samples had enough free carriers to dominate the absorption measurement, so that no information about the absorption band gap could be gathered. While the spectrum from the intrinsic samples showed a higher transmittance, it was still large enough to preclude accurate measurements of the band gap.

To overcome this problem we implemented a light source with a greater intensity, namely the optical parametric amplifier laser system. This presented another set of difficulties. One of the problems is that there is a fair amount of substrate absorption, as in the FTIR measurements. The $CdCr_2Se_4$ layer is also very thin (100 nm), and thus the photocurrent signal is very weak. Even when a measurement can be made, there is no guarantee that it is actually from the conduction band offset. As mentioned above there are a number of other absorption processes that can cause a photocurrent, including two-photon absorption, and defect absorption. As demonstrated two-photon absorption is more prevalent at higher intensities, but often when the intensity is low enough for two-photon absorption to be negligible, the signal is too small to be measured. The middle ground is very difficult to find.

The first photocurrent measurements taken were initially very noisy, but more importantly, the cause of the photocurrent was unknown. We were worried that the absorption came from non-linear effects, such as two-photon absorption, instead of exciting electrons across the band offset. To discover the cause, the power dependence

was measured, and noted to be greater than linear. This seemed to indicate that two-photon absorption was the dominant absorption process for our measurements. In order to decrease two-photon absorption, we decreased the intensity of the laser. As noted in equation 4, two-photon absorption is dependent on the peak intensity of the laser pulse. By decreasing the intensity of the pulse, such as by broadening the pulse, we could decrease the peak intensity. As two-photon absorption is non-linear, it would decrease faster than linear processes, and in this way we could try to remove it.

After the intensity was decreased the power dependence was again measured. As shown in figure 17, the power dependence at lower intensities was very close to linear. At higher intensities the material demonstrated non-linear dependence due to saturation. The intensity was then chosen in the linear regime to make two-photon absorption negligible. This allowed us to be sure that the photocurrent we were measuring was from electrons crossing from one conduction band to the other. In this way we were able to measure the conduction band offset. The experiment was then repeated on the paramagnetic sample, at this lower intensity.

The results of the second set of measurements are shown in figures 18 and 19. As noted previously, the band offset continues to increase with lower temperature. More importantly, it is noted that the band offset is very close to the band offset at higher intensities. From this it can be concluded that, even at higher intensities, two-photon absorption does not dominate the photocurrent threshold. This indicates that all of the measurements taken were in fact measurements of the band offset.

This information allows a confident comparison between the paramagnetic and

ferromagnetic sample's band offsets. Original measurements were made on both a ferromagnetic and a paramagnetic diode. It is noted that the band offset for both samples increase with a decrease in temperature. This is typical paramagnetic behavior. However when compared, it is noted that the change in band offset for the ferromagnetic diode is slightly smaller. This may be one of the few indications of the ferromagnetism of diode #11. The ferromagnetism allows some band splitting, which causes the band offset to increase more slowly. Even with this, however, the splitting is very small, and thus the ferromagnetic sample displays only a very small amount of ferromagnetic character.

It can be thus concluded that the ferromagnetism of sample #11 does affect the band offset. It can also be shown to be very slight. This is most likely due to a mixed interlayer between the $CdCr_2Se_4$ and the AlGaAs substrate that destroys most of the expected ferromagnetism. To test this, more samples would need to be grown, and the band offsets must be characterized for a larger number of diodes.

6. REFERENCES

[1] D.D. Awschalom, D. Loss, N. Samarth, Semiconductor Spintronics and Quantum Computation, (2002)

[2] G. A. Prinz, Science **282**, 1660 (1998).

[3] H. B. Zhao, Y. H. Ren, B. Sun, and G. Lüpke, A. T. Hanbicki and B. T. Jonker, Appl. Phys. Lett. 82, 2003, pp. 1422-4.

[4] G. Schmidt, D. Ferrand, L. W. Molenkamp, A. T. Filip, and B. J. van Wees, Phys. Rev. B **62**, R4790 (2000).

[5] Y. D. Park, A. T. Hanbicki, J. E. Mattson, and B. T. Jonker, Appl. Phys. Lett. **81**, 1471 (2002).

[6] P. K. Baltzer, H. W. Lehmann, and M. Robbins, Phys. Rev. Lett. **15**, 493 (1965).

[7] G. Harbeke and H. Pinch, Phys. Rev. Lett. **17**, 1090 (1966).

[8] A. Continenza, T. de Pascale, F. Meloni, M. Serra, PRB, 49, 2503 (1994)

[9] Q. Yang, B. Sun, H.B. Zhao, Y.H. Ren, G. Lüpke, A.T. Hanbicki, B.T. Jonker, Determination of conduction band offset at $CdCr_2Se_4/Al_xGa_{1-x}As$ interface by free carrier absorptioni-induced internal photoemission, handout, (2003).

[10] C. Kittel, Introduction to Solid State Physics, (1986).

[11] N. Sanford and S.J. Nettel JAP, 52, 3542, (1981).

[12] W.J. Miniscalo, B.C. McCollum, N.G. Stoffel, and G. Margaritondo, PRB, 25, 2947, (1982).

[13] Q. Yang, Electronic and magnetic properties of spinel semiconductor $CdCr_2Se_4$, presentation (2003)

[14] J. Miragliotta and D.K. Wickenden, Appl. Phys. Lett. 69, 14 (1996).

[15] S. P. Davis, M.C. Abrams, J.W. Brault, Fourier Transform Spectrometry, (2001).

[16] W. Silfvast, Laser Fundamentals, (1991)